Research Article

Study on W/(TiN)Ta composite and its application in shape charge liner

Zizhi Yan[1] · Gaoyong Xu[1] · Jinping Suo[1]

Received: 21 September 2019 / Accepted: 16 September 2020 / Published online: 25 September 2020

Abstract
In the present work, W/Ta and W/TiN/Ta laminated composites have been prepared by spark plasma sintering (SPS) and compared with W/W multilayer through three point bending and tensile tests. The results show that Ta has good reinforcing and toughening effect on W. The tensile strength of W/Ta is 371 MPa, and the three-point bending strength is 774 MPa, which are much higher than that of W/W. To further improve the mechanical property pf W/Ta, W-Ta laminated composites with TiN interlayer (W/TiN/Ta) has been studied. W/TiN/Ta have much higher strength than that of W/Ta due to intrinsic high strength of TiN and the increased layered interfaces, while worse ductility. Then, the feasibility of applying W/Ta laminated composite to the liner was tested by explosion overload test. The test results have been analyzed by Scanning Electron Microscope (SEM) and X-ray Diffraction (XRD). Explosion overload test results reveal that W/Ta laminated composite has the potential to be applied in shaped charge liner.

Keywords Tungsten laminated composites · Tungsten shaped charge liner · Composite shaped charge liner

1 Introduction

The shaped charge liners are widely applied in the modern ammunition and certain industries, e.g. oil, mining, geology, etc. [1, 2]. In many applications it is desirable for the jet to penetrate the target material to a depth as great as possible [3, 4]. According to the Szendrei formula which illustrated the factors influencing penetrate depth and hole diameter of metal jet: $H=(v_j-v_s)\cdot t_p\cdot(\rho_j/\rho_s)^{1/2}$ in which the H is the largest penetrate depth, the v_j and v_s is the metal jet head and bottom velocity, the t_p is the time before jet broken, the ρ_j and ρ_s is the density of shaped charge liner and target. From the formula we know that there are three ways to maximize the penetrate performance of jet: one is increasing the velocity gradient of jet, second is lengthening the time before jet broken and third is using high-density materials as the shaped charge liner [5].

However, as the velocity gradient increased the jet will break faster. In other words, the velocity gradient and the jet breakup time is incompatible. At present, the most effective method for maximizing penetration depth is to change the material used for the shaped charge liner [3]. That is to say, to increase the density of the material. In the past the liners for shaped charges have typically been composed primarily of wrought copper. But the density and melt point of copper is too low to reach the desirable penetrate depth. Recent years, the high density, high acoustic velocity, good thermal conductivity, and high dynamic fracture elongation rate make tungsten one of the most attractive candidate materials for shaped charge liner [6]. But the disadvantage of tungsten is high brittleness [7]. Since the jets of tungsten alloy liners will extremely quickly disperse after formation, the use of tungsten alloy liners have been greatly restricted at large standoff [8]. Though there is mass of reported research on improving the ductility of tungsten, it remains a difficult challenge. Up to now, three main methods have been widely investigated, alloying, tailoring the microstructure and forming tungsten composites [9].

✉ Jinping Suo, jinpingsuo@hust.edu.cn | [1]State Key Laboratory of Material Processing and Die and Mould Technology, School of Materials Science and Engineering, Huazhong University of Science and Technology, Wuhan 430074, China.

SN Applied Sciences (2020) 2:1736 | https://doi.org/10.1007/s42452-020-03517-0

In our team, we have done a lot of research on the toughening of tungsten by forming tungsten composites [10, 11]. We found that the refractory metal tantalum and tantalum alloys which have excellent comprehensive properties such as high density (16.6 g·cm^{-3}), high melting point (2996 °C) has good toughening effect on tungsten. Otherwise, tantalum and its alloys also have other good properties like high dynamic fracture property, moderate sound speed and arson, which make them ideal materials for shell of armor-piercing projectile and explosive forming ammunition [12]. W and Ta have good wettability and infinitely mutual solubility in liquid state. For that, W-Ta laminated composites may solve the brittleness of tungsten at room temperature and the dispersion of tungsten after forming jet. At room temperature, Ta can provide toughness to improve the processing properties of W composites. After forming a melt jet, Ta can prevent the dispersion of W jet.

So, we invented a W-Ta compound shaped charge liner. In order to form a steady metal jet, the following conditions must be reached: First, the composites must have enough strength and high dynamic fracture property to form a jet. Second, in the process of jet formation, W and Ta, which exist alone, must be fully mixed to prevent W from breaking. Due to the brittle phase formed by solid solution between W and Ta [13, 14], TiN coating with micro thickness was selected as the interlayer to prevent the direct contacting of W and Ta and further enhancing the interface bonding strength.

In this work, we prepared W/Ta and W/TiN/Ta laminated composites by SPS sintering technology. The mechanical properties of W/Ta and W/TiN/Ta have been tested. As W/TiN/Ta plasticity deteriorates, it does not meet expectations. So, only W/Ta laminated composite has been processed into a shaped charge liner to verify whether it can form a metal jet.

2 Study on mechanical properties of W-Ta laminates

2.1 Experimental procedure

The structure of W/TiN/Ta laminated composites is shown in Fig. 1. The tungsten and tantalum sheet with 0.1 mm thick stacked alternately and with TiN coating in the middle. The structure of W/Ta is similar with W/TiN/Ta, which without TiN interlayer. The tantalum and tungsten sheet were purchased from Tianshengtai Pioneer Metals Corporation, Baoji, China. The purity of tantalum and tungsten were 99.95%. Tantalum sheet was prepared by cold rolling, vacuum annealing at 1000 C for 1 h and then cooling with furnace; tungsten was prepared by hot rolling, vacuum annealing at 900 C for 1 h and then cooling with furnace. TiN coating was directly deposited on both sides of tantalum sheet by arc ion plating. The thickness of TiN coating is about 1 μm. Figure 2 a, b is the surface morphology of TiN prepared by arc ion plating. Figure 2c is the cross-sectional morphology. Table 1 shows the functions and characteristics of each components:

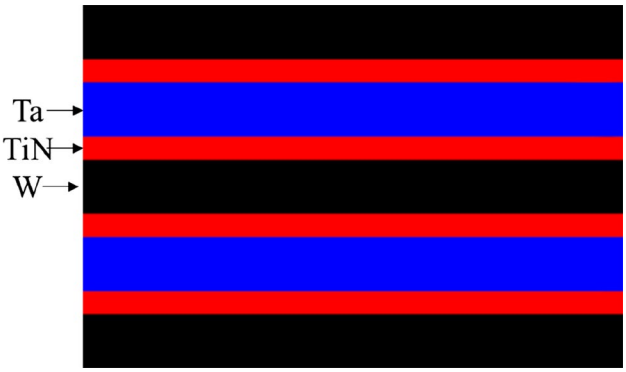

Fig. 1 The structure of W/TiN/Ta laminated composites

- W: high hardness, high melting point, high density, low plasticity;
- Ta: high melting point, high density, high plasticity;
- TiN: high melting point, high hardness, low plasticity, preventing W, Ta from forming brittle phase and strengthening the interface.

In this work, tungsten and tantalum wafers were cleaned by ultrasonic wave in acetone and alcohol for 5 min to remove the surface oil and then dried in a vacuum drying box. The number of tungsten and tantalum wafers per sample was 20 W + 19Ta (TiN) alternately stacked. The samples were sintered by SPS sintering furnace (sinter land, LABOX-1575) and the sintering was conducted at 1700 °C for 10 min under 60 MPa. The sintered specimens were then cut into tensile specimens for tensile tests and three-point bending specimens for three-point bending tests.

2.2 Tensile test results and analysis

Tensile test was carried out with a high temperature rupture tester. The tensile rate is 1 mm·min^{-1}. The dimension of the standard distance part of the specimen was 12 mm × 2.5 mm × 1.5 mm. The tensile specimen is shown in Fig. 3. Tensile fracture morphology was then observed by FEI Quanta200 Scanning Electron Microscope.

Figure 4 is the tensile stress–strain curve of various W-Ta laminates. As we can see in the figure, W/W laminates has a bad strength and toughness for its intrinsic brittleness.

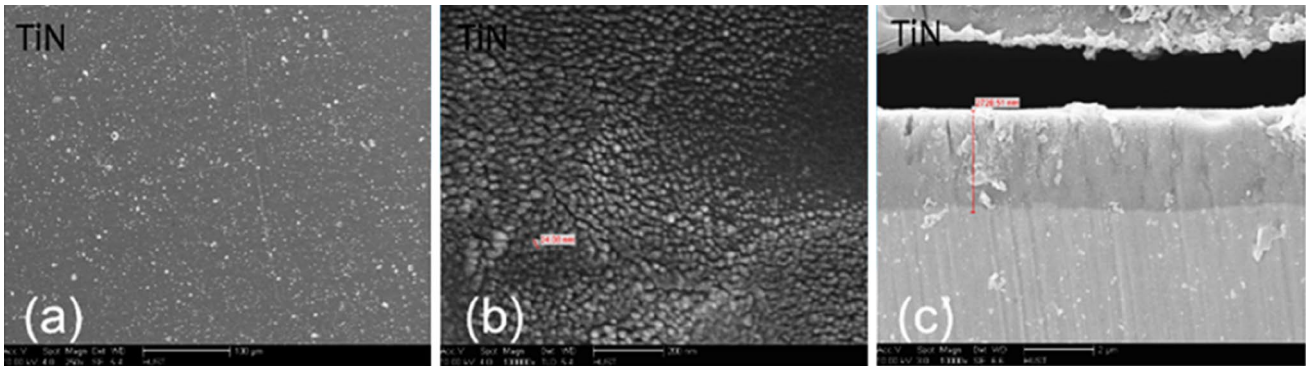

Fig. 2 Nano-TiN coating prepared by Arc Ion Plating **a, b** Surface topography **c** Cross-section morphology

Table 1 The properties of each components

	Density/ $g{\cdot}cm^{-3}$	Specific heat capacity/ $J{\cdot}kg^{-1}{\cdot}°C^{-1}$	Melting point/ °C	Mohs hardness	Tensile strength/ MPa
W	19.2	0.13×10^3	3422	7.5	35–1500
Ta	16.7	0.14×10^3	3017	6.5	350–500
TiN	5.22	–	2930	8-9	–

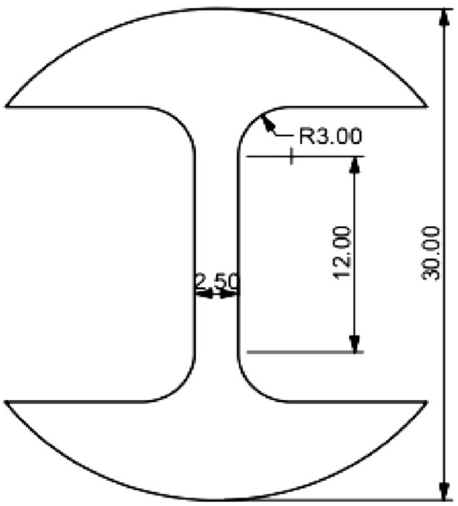

Fig. 3 Schematic diagram of tensile sample and the thickness is 1.5 mm

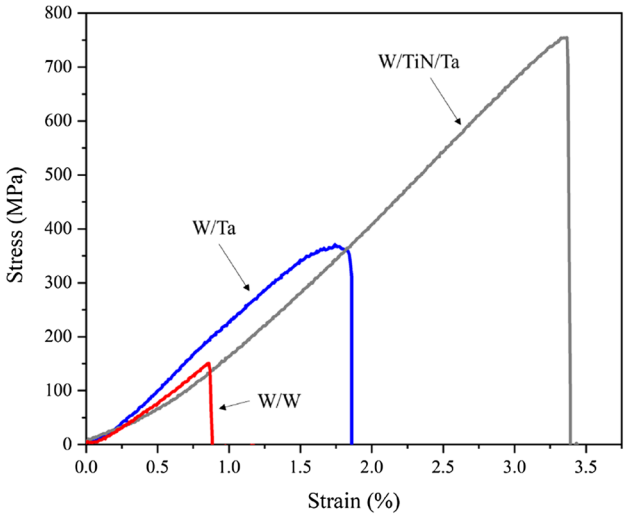

Fig. 4 Tensile stress–strain curve of various W/Ta laminates

Table 2 Tensile test properties of various W/Ta Laminates

Components	Strength (MPa)	Elongation (%)	Integration (MPa· %)
W/W	151	0.86	58.5
W/Ta	371	1.74	374.6
W/TiN/Ta	754	3.37	1173.9

Ta shows a strong toughening effect on W whose strength is higher than W/W. The strength of W/TiN/Ta has a high strength which beyond 750 MPa. Table 2 is the tensile test properties of various W/Ta Laminates. The strength and elongation of W/TiN/Ta is almost two times than of W/Ta, while the Integration (strength plastic integration) is almost 3 times.

Figure 5 is the tensile fracture morphology of various W/Ta Laminates, (a)(b) are W/W laminates with the low and high magnification fracture morphology, (c) and (d) are W/Ta and (e)(f) are W/TiN/Ta. From Fig. 5b we can see that the toughening effect of laminates is not reflected in W/W. The crack germinated and diffused in the matrix, and it continued to spread across the interface when it encountered the W/W interface. The fracture is smooth.

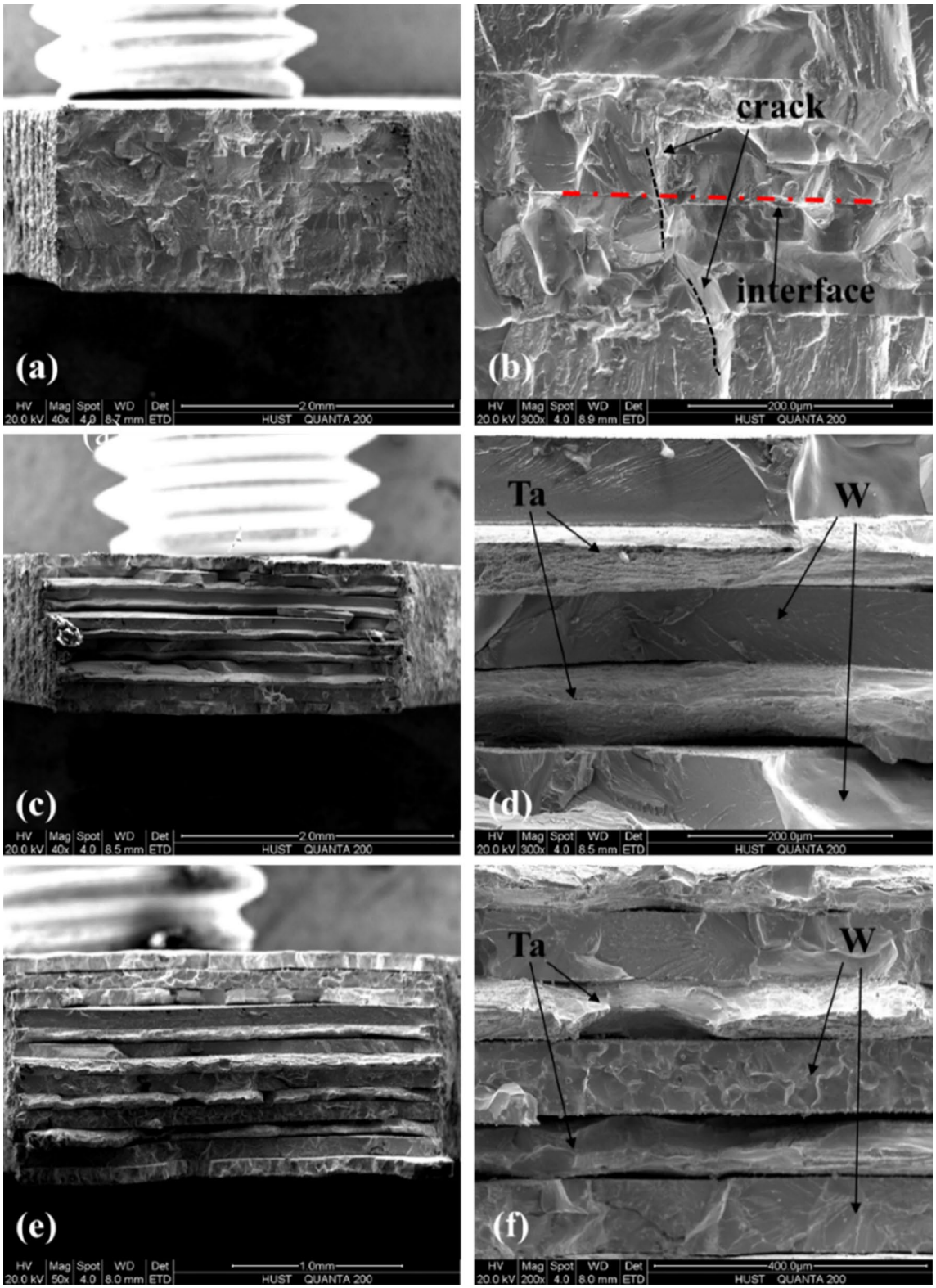

Fig. 5 Tensile fracture morphology of various W/Ta Laminates

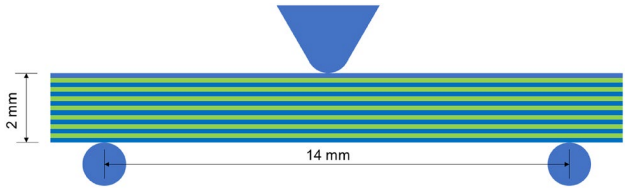

Fig. 6 Schematic diagram of three-point bending tests. The testing span was 14 mm, the height and width are 2 mm. The broadsides of the sample have been polished to observe the crack propagation

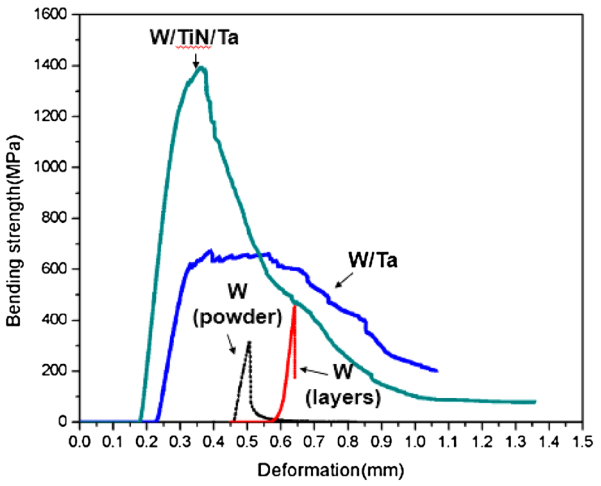

Fig. 7 Stress-strain curves of three-point bending of various W/Ta laminates

From Fig. 5c–f, we can find that the fractures are jagged. When the crack spreads to the interface, as the toughness of Ta, it can't continue to spread forward. Then it had to spread along the interface. Because of the interface and Ta, the mechanical properties of W/Ta composites are improved. And as the intrinsic high strength of TiN and the increased layered interfaces, W/TiN/Ta shows a higher strength and ductility than W/Ta.

2.3 Three-point bending test results and analysis

The three-point bending performance test used Zwick/Roell Z020 universal testing machine, and the indenter speed was 0.3 mm·min^{-1}. The sample size is 18 mm × 2.5 mm x 2 mm (long × width × height), and the span is 14 mm. Figure 6 is the schematic diagram of three-point bending tests. In order to observe the crack propagation, we prepared some samples whose broadsides have been polished and three-point bending test stopped when the load declined half of the maximum load. Three-point bending crack distribution and cross section were then observed by FEI Quanta200 Scanning Electron Microscope.

Figure 7 is the stress–strain curves of three-point bending of various W/Ta laminates. From Fig. 7 we can find that the results of three-point bending test are similar to the results of tensile test. W/TiN/Ta has a highest strength which reached to 1400 MPa. The strength of W/Ta is about 700 MPa, half the strength of W/TiN/Ta. But the fracture mechanisms are different. In Fig. 4, we can find that all the laminated composites broken quickly when the strength reached the highest value. In Fig. 7, however, when the load reached the highest value, the W/TiN/Ta broken and the load plunged. But from the Stress–strain curve of W/Ta, we can note that when the load reached the highest value, W/Ta didn't fail immediately. There is an evident yield platform before W/Ta failed.

Figure 8 are the crack propagations images in Ta/W and W/TiN/Ta. From Fig. 8, we can find that there are four different states during the crack propagates which marked with A, B, C and D. A means the initial crack. As the deformation of composites, W layer break firstly. As the existent of Ta layer, the tip of crack has been weakened. With the increase of load, the cracks begin to propagate into Ta. B means plastic deformation of Ta layer under external stress. C means the failure of Ta layer. D means propagation of cracks along the interface, it can lead to interfacial peeling.

We know that the toughening of composites is the four mechanism. (1) plastic deformation of toughened layer. (2) crack tips weaken. (3) crack deflection. (4) interface de-bonding. From Fig. 8a, we can find that there are a lot of regions A which lay on front and nearby of the crack propagation path. This means that a large number of crack tips have been effectively weakened. In Fig. 8b, the mark B shows that plastic deformation of Ta layer has occurred on crack propagation path, which delayed the fracture of W/Ta and lead to the emergence of yield platforms. The debonding of interface also can be observed in Fig. 8b. This can lead to crack deflection and dissipation of energy. The emergence of A, B, D are advantage for the toughening of W/Ta.

Compared with Fig. 8c, d and a, b, we can find that the fracture mode of W/TiN/Ta is different from that of W/Ta. In Fig. 8c we can only find one region A. Once W layer broken, the crack will propagate into Ta layer quickly and leading the failure of laminated composites. The Ta layer cannot dissipate enough energy to weaken the crack tip as the load is too large and the crack propagation speed is too fast. This also can be observed in Fig. 8d. Ta layers have no obvious plastic deformation process, but fracture directly. Another thing should be noted is that the interface bonding of W/TiN/Ta is bad. In Fig. 8c, we can see that in the middle of the composite, the interface is completely debonded along a layer.

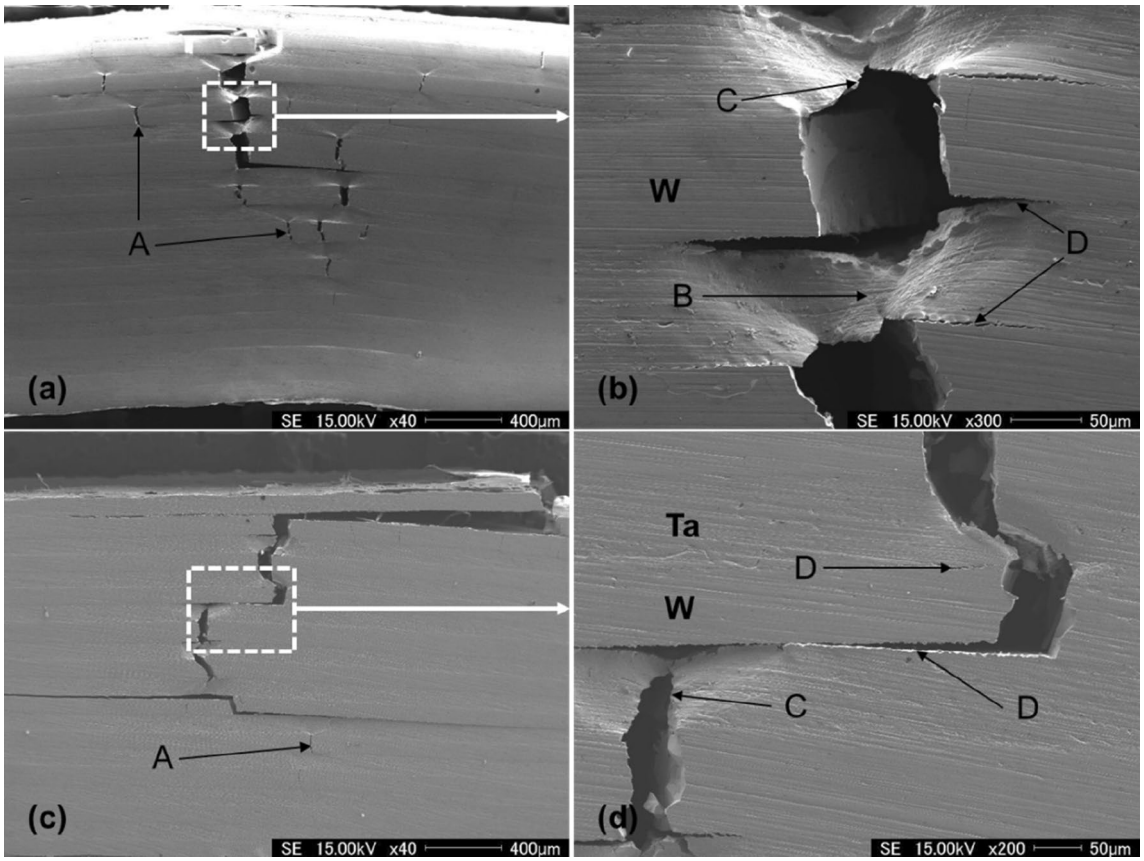

Fig. 8 Crack propagations images in Ta/W **a, b** and W/TiN/Ta **c, d** laminated composites

Above all, we concluded that Ta has a good toughening effect on W by crack tips weaken, crack deflection by interface debonding and dissipation of energy by plastic deformation. The TiN coating can improve strength greatly but bad for the bonding of W/Ta interface and worsen the plastic of W/Ta.

3 Study on the feasibility of applying tungsten composite to the liner

3.1 Experiment procedure

In order to verify whether W-Ta composite can be applied in shaped charge liner, a W-Ta compound liner has been prepared. For the bad ductility and interface bonding of W/TiN/Ta, only W/Ta compound liner was prepared. The structure of W/Ta compound liner is shown in Fig. 9.

The explosion overload test conditions are shown in Table 3. The diameter of shaped charge liner is 29.18 mm; the height is 17.72 and wall thickness is 1.78 mm. The height of cylindrical powder pellet is 46 mm and its quality is 58 g. The stand-off distance is 90 mm.

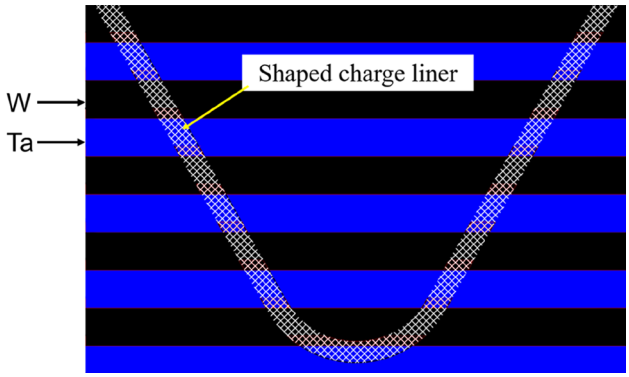

Fig. 9 Structure of W/Ta compound liner

3.2 Test results and analysis

Figure 10 is the result of explosion overload test. Metal jet formed a penetration hole on the steel target with a hole size of 10.3 mm × 6.5 mm and a depth of 28.5 mm. From Fig. 10b we can see that the hole was formed by the typical jet penetration. The hole has a big entrance

Table 3 The explosion overload test conditions

Size of shaped charge liner			Cylindrical powder pellet(JH-2)		Stand-off distance
Diameter	Height	Wall thickness	Height	Quality	90 mm
Φ29.18 mm	17.72 mm	1.78 mm	46 mm	58 g	

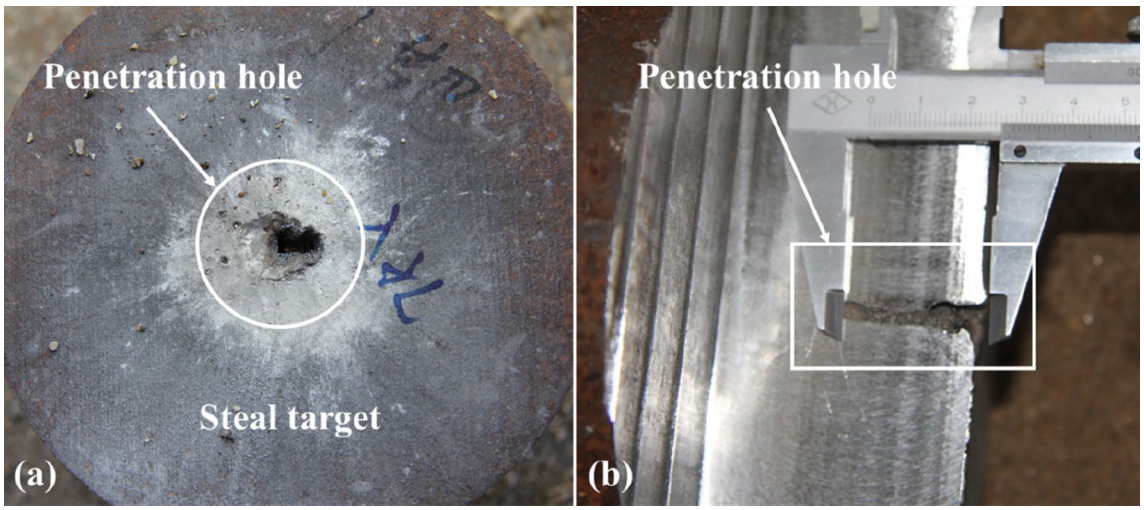

Fig. 10 The result of explosion overload test

aperture and a uniform aperture in the middle and a bigger aperture in the bottom.

Figure 11 are the SEM images of the inner wall of penetrating hole and the components distribution of Ta、W and Fe. From Fig. 9 we can find that the distribution of Ta and W are absolutely coincident. However, as mentioned earlier, W and Ta exist alone. As we known, W and Ta have good wettability and infinitely mutual solubility in liquid state. therefore, one possible explanation is that during the formation of the metal jet, W and Ta are fully mixed in relatively big area of hundreds of micrometers. This indicates that the temperature of the jet may be close to the melting point of tungsten (3422 °C) during penetrating into the target.

Figure 12 is the XRD diffraction pattern of the inner wall of the penetrating hole. XRD analysis showed that the main components of the inner wall of the penetration hole were the oxides of Ta, carbides of Ta, WTa compounds, matrix Fe and its oxides. We can also find that there is an amorphous diffraction peak at the angle of about 16°. Combining the previous results, we can conclude that the amorphous material is formed by the rapid cooling of the liquid WTa jet after penetrating the target plate. This also proves that the W/Ta compound shaped charge liner can form a metal jet.

4 Conclusion

In this paper, we use Ta to toughen W and prepared W/Ta composites with better mechanical properties than W/W and W powder material. A novel type of tungsten based composite liner structure is also presented. The following conclusion can be made.

1. The W/Ta composites fabricated by SPS have good mechanical properties. Tensile strength reached 371 MPa. Ta shows strong toughening effect on W.
2. As the interface of W-Ta, TiN coating greatly improves the mechanical properties of W-Ta composites. Tensile and three-point bending strength of W/TiN/Ta reached 754 MPa and 1400 MPa, respectively. But the ductility and interface bonding of W/TiN/Ta become worse.
3. W/Ta composite liner can form a metal jet. During the formation of the metal jet, the temperature reached above the solution point of tungsten, and the tungsten and tantalum melted and fully mixed. This is an important basis for forming a metal jet with a W/Ta composite shaped charge liner.

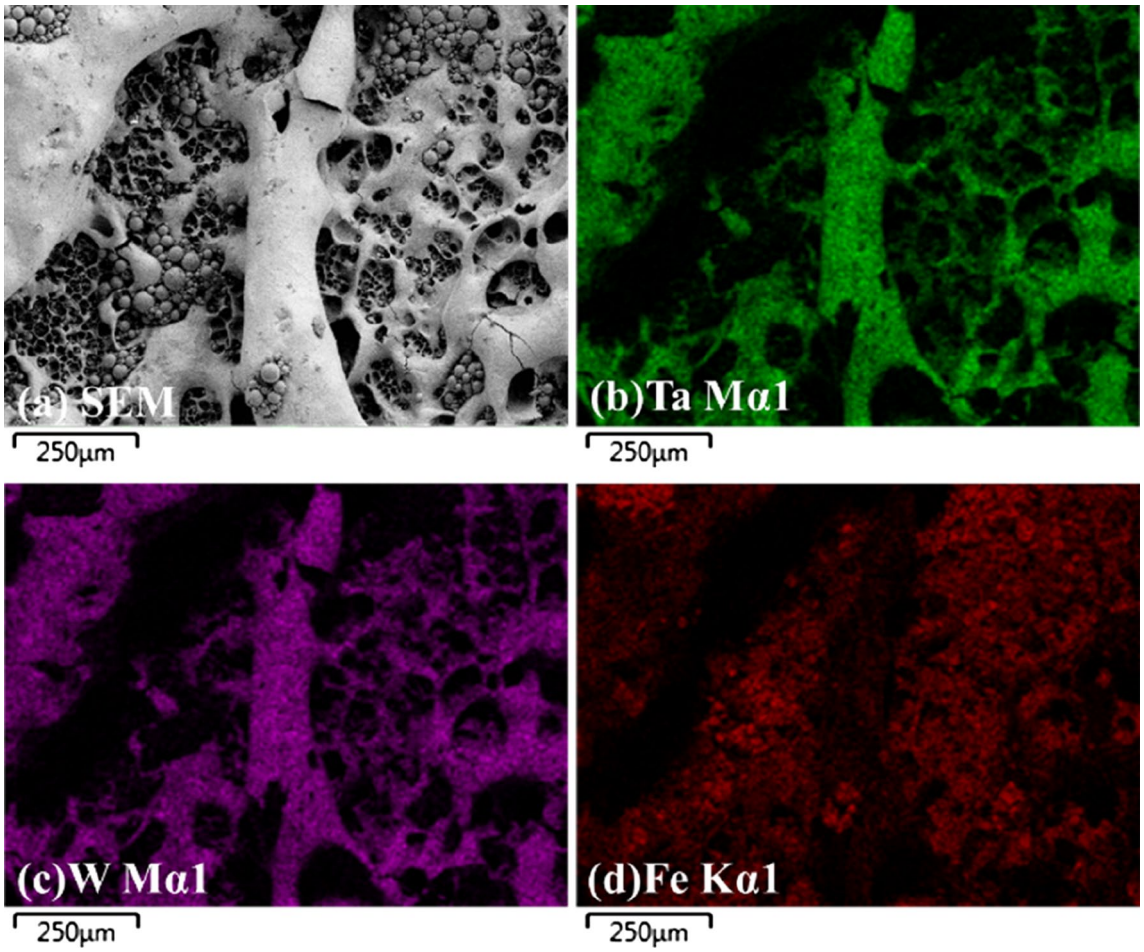

Fig. 11 The SEM image of the inner wall of penetrating hole and components distribution of Ta, W and Fe

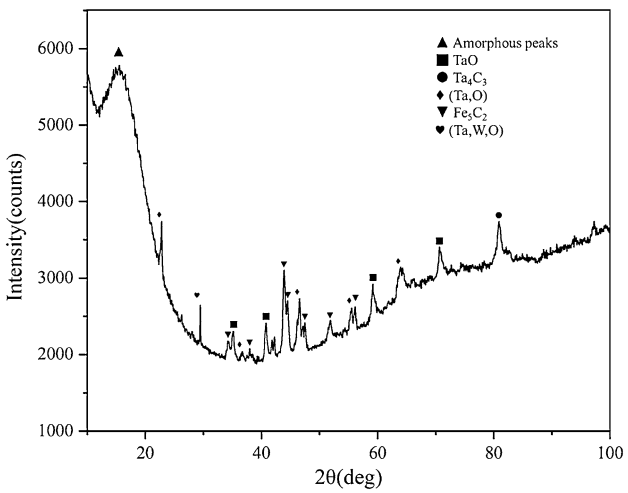

Fig. 12 The XRD diffraction pattern of the inner wall of the penetrating hole

Acknowledgements This research work is funded by The National Natural Science Foundation of China.

Funding This study was funded by The National Natural Science Foundation of China (11875030).

Compliance with ethical standards

Conflict of interest The authors declare that they have no conflict of interest.

References

1. Walters W (2007) Introduction to shaped charges. Army Research Laboratory
2. Wang T-F, Zhu H-R (1996) Copper-tungsten shaped charge liner and its jet. Propellants, Explos, Pyrotech 21:193–196
3. He Hanwei, Jia Shouya (2010) Direct electrodeposition of Cu-Ni-W alloys for the liners for shaped charges. J Mater Sci Technol 26(5):429–432
4. Saran Salih et al (2013) Experimental investigations on aluminum shaped charge liners. Procedia Eng 58:479–486

5. Zernow L (1997) The density deficit in stretching shaped charge jets. Int J Impact Eng 20:849–859
6. Wang T, Zhu H, et al. (1992) Copper-tungsten shaped charge liners and their performance. J Ballist 2:61–66
7. Hirai T et al (2015) Status of technology R&D for the ITER tungsten divertor monoblock. J Nucl Mater 463:1248–1251
8. Dong Wen-Jian, Liu Jin-Xu, Cheng Xing-Wang et al (2016) Penetration performance of W/Cu double-layer shaped charge liners. Rare Met 35(2):184–191
9. Bonk S, Reiser J, Hoffmann J, Hoffmann A (2016) Cold rolled tungsten (W) plates and foils: evolution of the microstructure. Int J Refract Metals Hard Mater 60:92–98
10. Zhang Y, Ouyang T, Suo J et al (2016) Effect of thickness ratio on toughening mechanisms of Ta/W multilayers. J Alloys Compd 666:30–37
11. Zhang Y, Xu G, Suo J et al (2017) Mechanical properties study of W/TiN/Ta system multilayers. J Alloys Compd 725:283–290
12. Walters W et al (2001) The penetration resistance of a titanium alloy against jets from tantalum shaped charge liners. Int J Impact Eng 26:823–830
13. Makhlai VA et al (2015) Damaging of tungsten and tungsten–tantalum alloy exposed in ITER ELM-like conditions. J Nucl Mater 463:1248–1251
14. Tejado E et al (2015) The effects of tantalum addition on the microtexture and mechanical behavior of tungsten for ITER applications. J Nucl Mater 467:949–955